

# Full-arch intraoral scanning: comparison of two different strategies and their accuracy outcomes

► F. MANDELLI<sup>1</sup>, E. GHERLONE<sup>2</sup>, A. KEELING<sup>3</sup>, G. GASTALDI<sup>4</sup>, M. FERRARI<sup>5</sup>

<sup>1</sup> Oral Science Dept. Vita Salute IRCCS – San Raffaele University Milan, Italy - Department of Fixed Prosthodontics

<sup>2</sup> Head Director Dental School, Vita-Salute University, Milan, Italy and Department of Dentistry, IRCCS San Raffaele Hospital, Milan, Italy

<sup>3</sup> Clinical Associate Professor in Restorative Dentistry, Leeds School of Dentistry, University of Leeds, UK

<sup>4</sup> MD, DMD, Associate Professor, Dental School, Vita-Salute San Raffaele University, Milan, Italy and Unit of Oral and Maxillofacial Surgery, San Rocco Clinical Institute, Ome, Brescia, Italy

<sup>5</sup> Chair, Department of Prosthodontics & Dental Materials, School of Dental Medicine, University of Siena, Italy

Professor, Department of Restorative Dentistry, School of Dentistry, University of Leeds, UK

Research Professor, Department of Restorative Dentistry, School of Dental Medicine, TUFTS University, Boston, USA

## TO CITE THIS ARTICLE

Mandelli F, Gherlone E, Keeling A, Gastaldi G, Ferrari M. Full-arch intraoral scanning: comparison of two different strategies and their accuracy outcomes. *J Osseointeg* 2018;10(3):65-74.

DOI 10.23805 /JO.2018.10.03.01

**KEYWORDS** Accuracy, Intraoral digital impression, Intraoral scanning, Precision, Trueness.

## ABSTRACT

**Aim** To test if there is a difference in accuracy between full-arch scans performed as two separate halves and stitched together, or as one continuous scan from side to side.

**Materials and Methods** A reference model with six implants was milled as a single titanium block. Six scan bodies were manufactured and screwed into the implants. A reference 3D model was created using an industrial optical scanner. The experiment was performed using the same intraoral scanning machine (3M True Definition Scanner). The 'Stitching' strategy had the scan started from #27 to #13; after saving this part, the same procedure was performed from #17 to #23 and the software stitched the two halves automatically. The 'No Stitching' strategy had the scan performed as a single procedure. Using engineering software, six copies of the scan body CAD file were substituted to the six scan bodies of the RM and the centre point of each one was determined. Linear measurements were made between the detected points; mean distance and standard deviation were calculated for each of the fifteen measurement sets created.

**Results** Stitching and No Stitching did not show statistically significant differences (Stitching=0.0396 mm  $\pm$ 0.0409 mm, No Stitching=0.0452 mm  $\pm$ 0.0481 mm,  $p=.338$ ) but they differed significantly comparing absolute errors (Stitching=0.0442 mm  $\pm$ 0.0358 mm, No Stitching=0.0555 mm  $\pm$ 0.036 mm,  $p=.015$ ).

**Conclusions** Stitching showed a better precision compared to No Stitching, exhibiting a smaller standard deviation and a higher error density closer to zero.

## INTRODUCTION

Implant structures should fit passively to reduce tension between fixtures, in order to improve the success rate of implants and prostheses during function (1). A misfit of the structure can lead to mechanical complications, such as retention screw loosening or fracture, implant fracture or biological complications such as bone resorption around the fixtures and mucositis/perimplantitis caused by an increase in plaque retention (2). Nevertheless a zero misfit is nearly impossible to achieve because of the multiple working steps involved in producing a framework and misfits up to 280 microns have been reported (3). Luckily, a biological tolerance does exist (4, 5) and a 150-micron misfit is likely to be tolerated (6) Furthermore, a difference between the misfit found in in vitro studies and in vivo studies is expected (3).

A review of the literature (7) underlined that the accuracy of the impression, being the first step of the manufacturing process, is the main factor influencing the structures' fit. This accuracy depends upon impression material, impression technique, implant angulation and the number of implants (7).

Intraoral scanners (IOSs) were introduced more than twenty-five years ago (8) and their indications have expanded from single crowns to multiple-units bridges. Several articles have evaluated intraoral digital impressions and digital workflows, reporting reliable results for single crowns (9-14) and short bridges (15-19), but not yet for full-arches (20-23). Dental implant impressions can be made using scanbodies,

devices specifically designed in order to facilitate the intraoral scan. In the laboratory, the design software automatically registers the IOS scanned image of these bodies to their computer aided designed (CAD) facsimiles. This process recovers the three-dimensional position (and orientation) of the fixtures. Concerns about the fitting of the scan-bodies have been raised (24), but they refer to the manufacturing process and not to the underlying workflow. The described procedure is predictable for single implants (25, 26), but errors preventing an acceptable fit have been reported, even when using only two implants (27) captured with parallel confocal still imaging technology. Papers regarding digital impressions of full-arch, multiple implants agree that accuracy decreases when measuring the distance between fixtures placed on posterior teeth of opposite quadrants (28-30) but the error reported can vary from 23  $\mu\text{m}$  (29) to 497  $\mu\text{m}$  (31). Many authors agree on the fact that accuracy is influenced by confounding factors such as saliva, reflective surfaces, compliance of the patient, limited intraoral space, etc (10, 18, 20, 23, 27, 32, 33), but only a few investigated the software that controls the hardware (31) and scanning strategy (34). Furthermore, the impact of software and scanning strategy on the accuracy of the scan should be tested for each IOS model.

The aim of the present study was to test if there is a difference in accuracy between full-arch scans performed as two separate halves and stitched together, or as one continuous scan from side to side, performed with the same IOS based on active wavefront sampling technology. The null hypothesis was that there is a difference between the two scanning techniques.

## MATERIALS AND METHODS

### Master model

A titanium reference model (RM) of an edentulous upper jaw was fabricated (grade 5 Ti 6Al4V) using an anonymised impression of a patient stored in an exocad database. The patient had six internal connection implants placed (Winsix K implant, 3,8 mm diameter) and the implant platforms were directly milled in the RM during the manufacturing process in order to prevent possible micro-movements. This case was chosen because fixtures were placed at sites 17, 15, 13, 23, 25, 27, representing a long-span, full-arch rehabilitation with implants inserted at different depth and angulations. Six scan bodies were manufactured (Winsix K implant, 3,8 mm diameter) and screwed into the implants with a torque controlled-wrench at 15 N/cm. The model was lightly dusted with titanium oxide powder (LAVA Scan powder; 3MESPE) before the scanning procedure.

### Reference scan

The model was scanned with an industrial optical

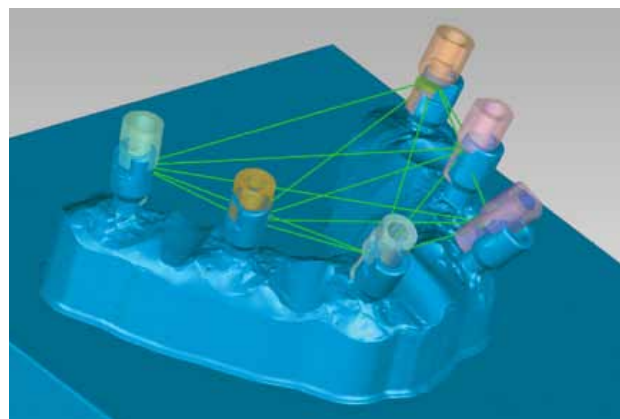


**FIG. 1** Representation of the study model: Titanium reference model is coloured in blue, CAD files of the scan abutments are superimposed and green lines represent all the measurements made. Misalignment between the reference model and scan bodies was created for illustrative purposes only.

scanner (ATOS II, GOM Braunschweig), a high-end machine previously used by other workers (13, 16), and a reference 3D object was created and exported in standard tessellation language (.stl) format. Three scans were performed and the mean values for each segment were used as a reference (Figure 1).

### Impression procedure

All the impressions were performed by the same experienced investigator (FM) who had performed more than three hundred scans with IOSs. All the scans were performed with the same IOS device (3M True Definition Scanner, Scanning Software 4.0.3.1; 3M ESPE).

In this experiment two different full-arch scanning strategies were tested.

1. Strategy with stitching (S): the optical device was firstly kept parallel to the occlusal plane and moved from the distal of #27 to the mesial of #13; it was then moved back to #27, tilting it toward the palatal side; the occlusal plane was crossed toward the buccal side and the camera was moved again from #27 to #13 trying to keep it orthogonal to the occlusal plane. The image was then inspected and missing regions were filled. The 3D scan was saved and the same procedure was performed with the other half of the model, from the distal of #17 to the mesial of #23. The software automatically applied a stitching algorithm in order to merge the two halves, based on the area between #23 and #13, shared by both the separate scans. The resulting 3D scan of the full arch was then exported in the standard tessellation format (.stl).
2. Strategy with no stitching (NS): the optical device was firstly kept parallel to the occlusal plane and moved from the distal of #27 to the distal of #17; it was then moved back to #27, tilting it toward the

Strategy	error (mm)	std. dev (mm)	p-value	abs error (mm)	std. dev (mm)	p-value
Stitch	.0396	.0409	.338	.0442	.0358	.015*
NoStitch	.0452	.0481		.0555	.0355	

TABLE 1 Global comparison of the two tested techniques.



FIG. 2 Distribution of absolute errors (in millimetres). Box plot: bottom edge of the box is the first quartile, horizontal line is the median, centre of the diamond is the mean, upper edge of the box is the third quartile; Red bracket denotes the “densest” region of the data. Absolute errors of the Stitch strategy have a tendency to be more concentrated and closer to zero.

palatal side, then finally forward from the distal of #27 to the distal of #17 toward the buccal side. The image was then inspected and missing regions were filled. The resulting 3D scan of the full arch was then exported in the standard tessellation format (.stl).

For all the scans, an approximate 80% registration of each scan body was considered sufficient to accept the scan.

Ten scans were performed for each tested strategy.

### Data processing

Using an engineering software (Geomagic Studio 2013) six copies of the scan body CAD file (the project used to produce the used scan bodies) were aligned and substituted to the six scan bodies of the RM and the centre point of each one was determined. Linear measurements were made between the detected points as shown in Figure 1. Mean distance and standard deviation were calculated for each of the fifteen measurement sets created. Each segment could be either larger or smaller than the reference distance: since summarizing data with mean values only could have led to overestimating accuracy (because positive and negative errors tend

to eliminate each other), errors of the distances were further analyzed as absolute values. Errors were further divided by the length of their reference segment to obtain an error percentage.

### Statistical analysis

Data were analysed using statistical software (IBM SPSS v.21). Independent samples t-test was used to evaluate overall trueness differences between group S and group NoStitch; Independent samples t-test with Holm’s correction for multiple comparisons was used to test each one of the fifteen segments. Spearman’s rank-order correlation was used to investigate correlations between errors, segment length and segment position.

## RESULTS

Data were normally distributed except for NoStitch, segment 27-23 (Shapiro-Wilk’s  $p = .036$ ) and for S, segment 27-16 (Shapiro-Wilk’s  $p = .034$ ). With global comparison as seen in Table 1, Figure 2, S and NoStitch did not show statistically significant differences ( $S = 0.0396 \text{ mm} \pm 0.0409 \text{ mm}$ , NoStitch =  $0.0452 \text{ mm} \pm 0.0481 \text{ mm}$ ,  $p = .338$ ) but they differed significantly comparing absolute errors ( $S = 0.0442 \text{ mm} \pm 0.0358 \text{ mm}$ , NoStitch =  $0.0555 \text{ mm} \pm 0.036 \text{ mm}$ ,  $p = .015$ ).

Results regarding the length of each one of the 15 segments are given in Table 2 and in Figures 3 to 6.

S and NoStitch showed similar results, except for segment 13-15, where S showed significantly better results for absolute error ( $p = .003$ ).

Correlation analysis showed statistically significant positive correlation between error/absolute error and reference length and between error percentage/absolute error percentage and segment position; no correlation was found between error/absolute error and segment order (Table 3).

## DISCUSSION

The aim of this study was to evaluate if there is a difference between two different scanning strategies for a full-arch implant impression; our null hypothesis was that there is a difference between the two strategies and it was rejected. Our results were in contrast with a previous study (34), but a newer machine was used. Both the tested strategies were suggested by the

manufacturer and linear measurements, instead of global deviations were evaluated. For these reasons it is hard to compare our results to the aforementioned study. Our results were also similar to a previous study (29) that tested three different IOSs scanning a model in which three implants were placed in position of 46, 41 and 36; nevertheless, we simulated a fully edentulous patient, representing a more difficult scenario compared to the aforementioned study because of the lack of tooth surfaces as reference background. Even though S and NS showed similar results, S showed a better precision compared to NS, exhibiting a smaller

standard deviation and a higher error density closer to zero as seen in Figure 2. From a clinical perspective this is an important aspect, because the option of making a full-arch scan as two separate halves was not only demonstrated to be at least equivalent to a continuous scan, but also produced a smaller spread of the errors and a trend towards a better result overall.

Although carried out in an *in vitro* setting, decreasing the clinical applicability of our results, we think that they may impact on the clinical situation. Previous studies remarked that contingent factors such as saliva, reflective surfaces, compliance of the patient, limited spacing (10,

segment	strategy	error (mm)	std. dev (mm)	p-value	abs error (mm)	std. dev (mm)	p-value
27-25	Stitch	.0049	.0116	1.000	.0101	.0067	1.000
	NoStitch	-.0013	.0147		.0118	.0077	
27-23	Stitch	.0074	.0269	1.000	.0236	.0122	1.000
	NoStitch	.0336	.0424		.0451	.0276	
27-13	Stitch	.0459	.0228	1.000	.0459	.0228	1.000
	NoStitch	.0604	.0500		.0669	.0394	
27-15	Stitch	.0179	.0266	1.000	.0236	.0208	.360
	NoStitch	.0260	.0650		.0585	.0330	
27-17	Stitch	.0928	.0453	1.000	.0928	.0453	1.000
	NoStitch	.0683	.0769		.0903	.0439	
25-23	Stitch	-.0039	.0201	1.000	.0171	.0094	.709
	NoStitch	.0306	.0472		.0446	.0320	
25-13	Stitch	.0314	.0200	1.000	.0314	.0200	.780
	NoStitch	.0535	.0449		.0605	.0332	
25-15	Stitch	.0093	.0251	1.000	.0213	.0145	.469
	NoStitch	.0248	.0522		.0480	.0281	
25-17	Stitch	.0836	.0295	1.000	.0836	.0295	1.000
	NoStitch	.0684	.0568		.0766	.0431	
23-13	Stitch	.0529	.0195	1.000	.0529	.0195	1.000
	NoStitch	.0491	.0146		.0491	.0146	
23-15	Stitch	.0421	.0191	1.000	.0421	.0191	1.000
	NoStitch	.0474	.0207		.0474	.0207	
23-17	Stitch	.1075	.0237	1.000	.1075	.0237	1.000
	NoStitch	.0983	.0303		.0983	.0303	
13-15	Stitch	-.0015	.0101	1.000	.0073	.0067	.003*
	NoStitch	.0155	.0296		.0300	.0111	
13-17	Stitch	.0558	.0234	1.000	.0558	.0234	1.000
	NoStitch	.0654	.0377		.0671	.0340	
15-17	Stitch	.0488	.0184	1.000	.0488	.0184	1.000
	NoStitch	.0378	.0241		.0393	.0211	

TABLE 2 Segment comparison of the two tested techniques.

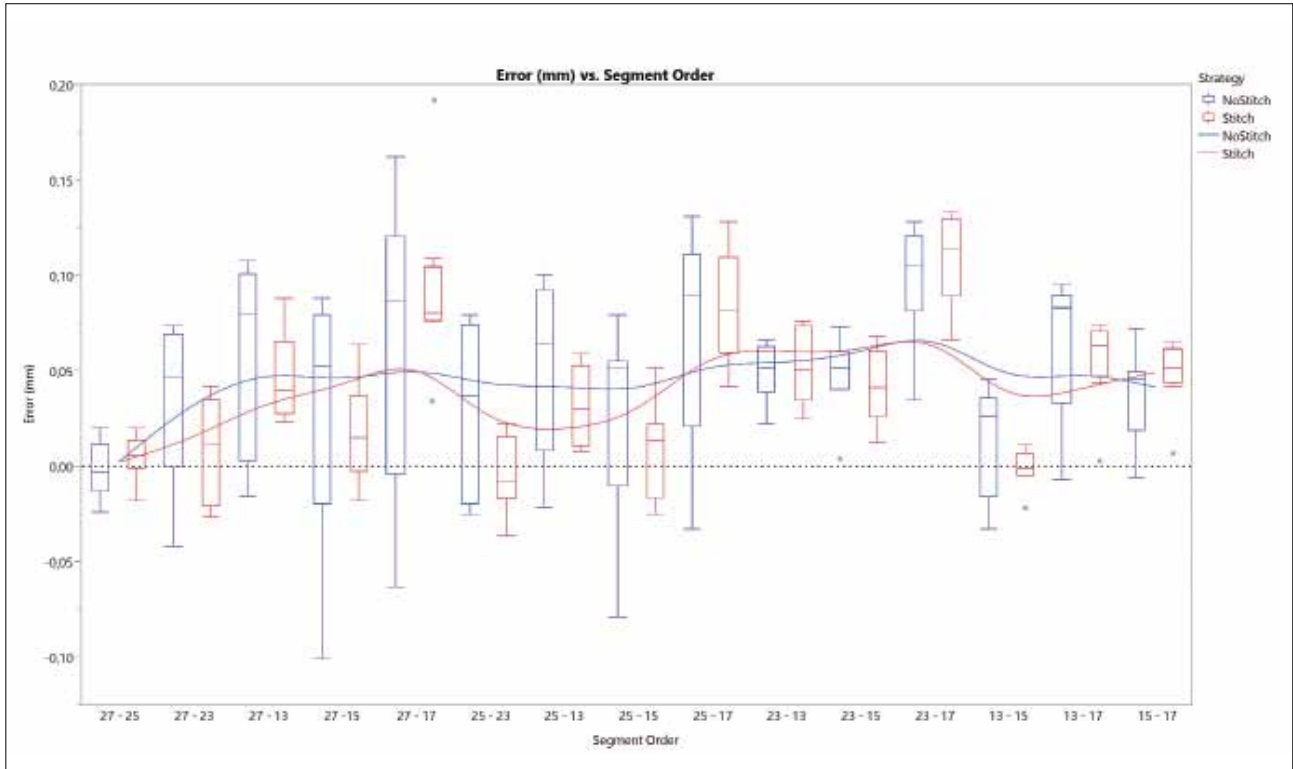


FIG. 3 Box plots and smoother lines (lambda = 0,05) illustrating errors (in millimetres) for each one of the 15 segments measured. Segments are ordered from left quadrant to right quadrant.

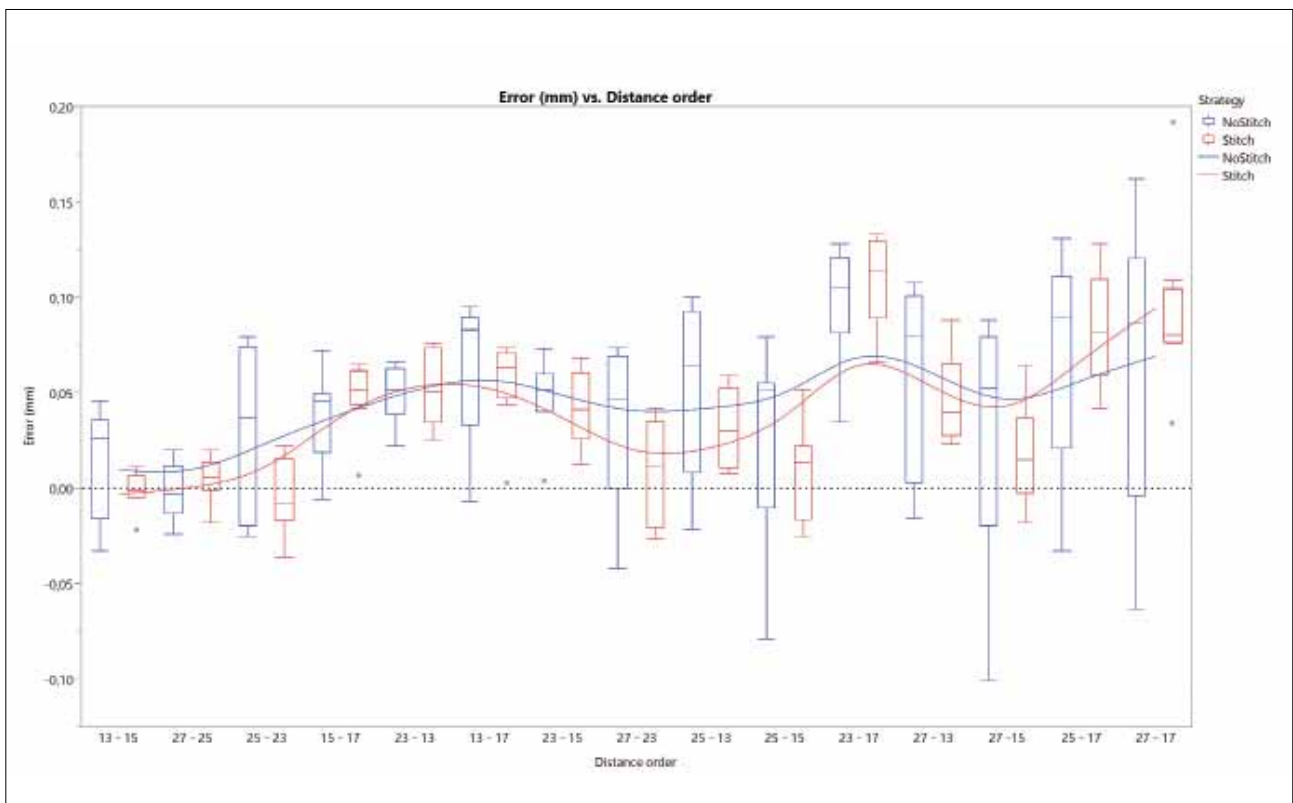


FIG. 4 Box plots and smoother lines (lambda = 0,05) illustrating errors (in millimetres) for each one of the 15 segments measured. Segments are ordered from the shortest (13-15 = 11,577 mm) to the longest (27-17 = 46,599 mm).

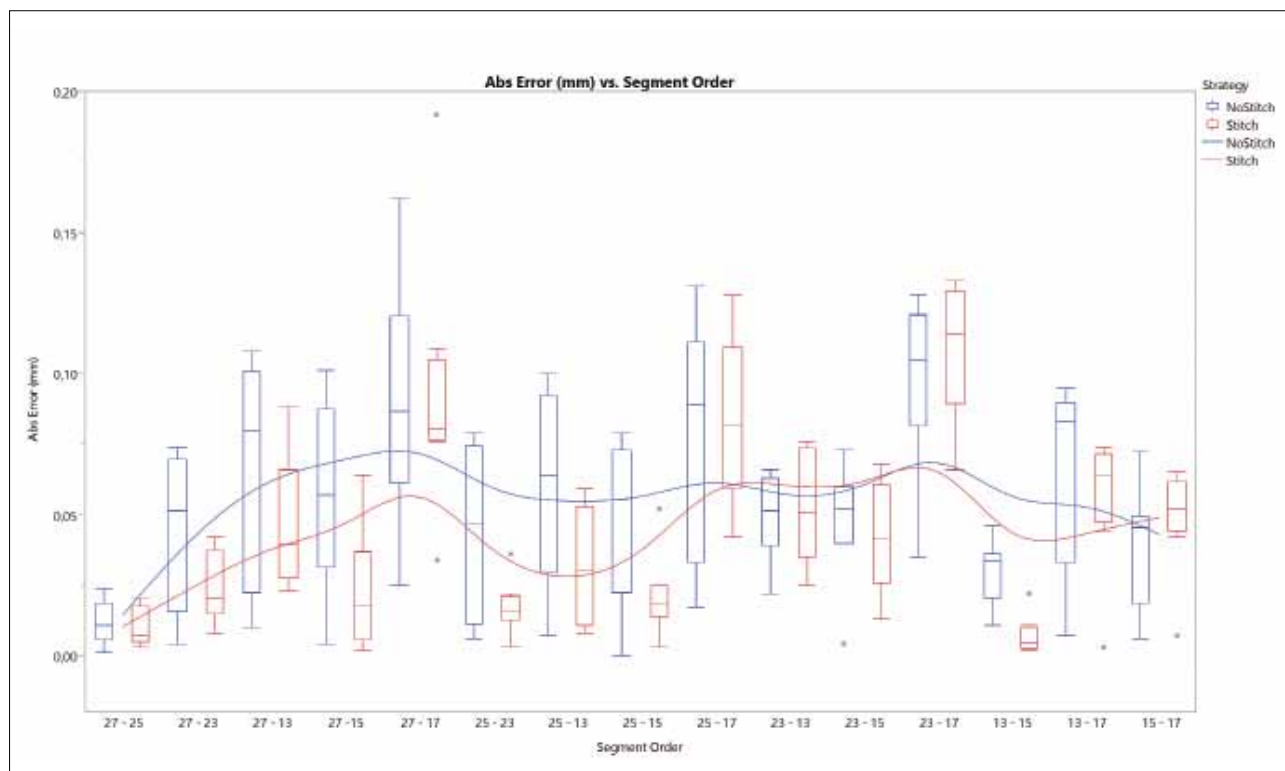


FIG. 5 Box plots and smoother lines ( $\lambda = 0,05$ ) illustrating absolute errors (in millimetres) for each one of the 15 segments measured. Segments are ordered from left quadrant to right quadrant.

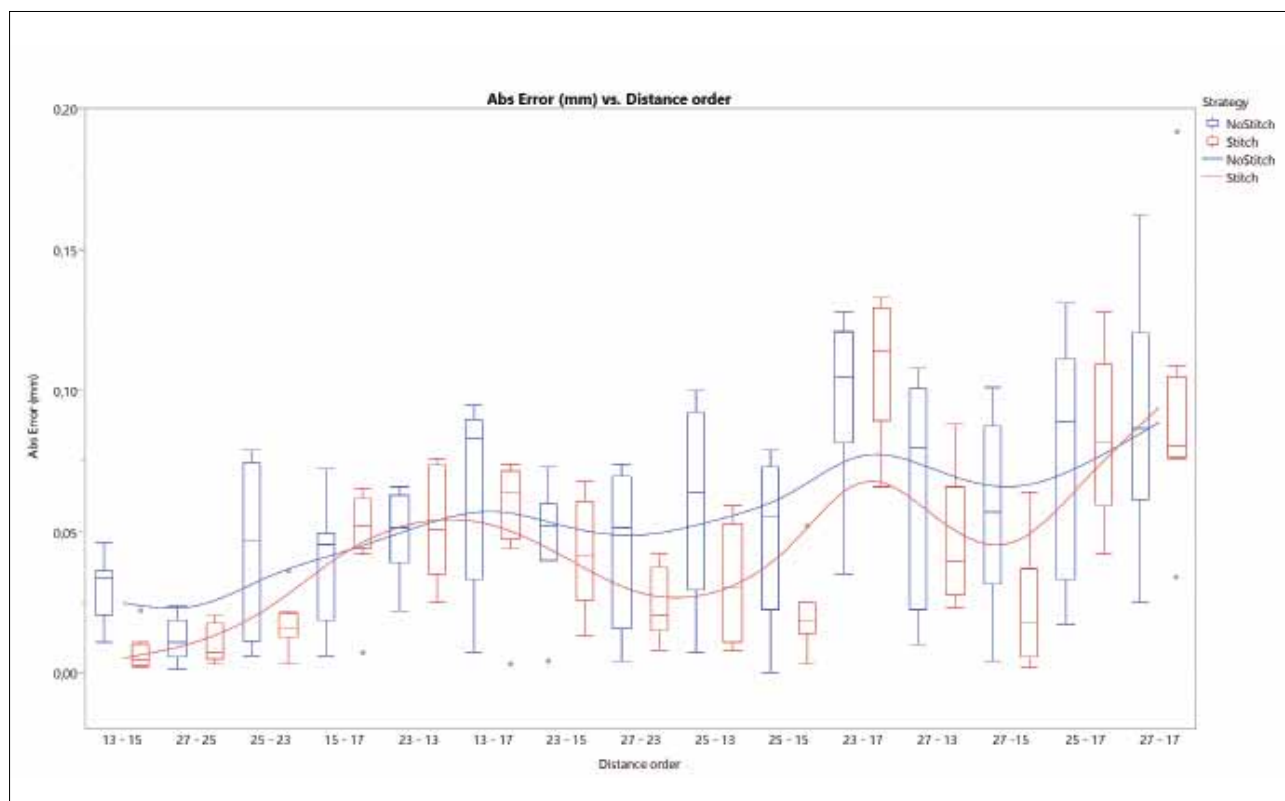


FIG. 6 Box plots and smoother lines ( $\lambda = 0,05$ ) illustrating absolute errors (in millimetres) for each one of the fifteen segments measured. Segments are ordered from the shortest (13-15 = 11,577 mm) to the longest (27-17 = 46,599 mm).



Variable	by Variable	Spearman $\rho$	Prob> p	Reference Figure
Segment order	Error (mm)	0,2483	0,0001*	Figure 3
Segment order	Abs Error (mm)	0,2381	0,0003*	Figure 5
Segment order	Error / Distance	0,4509	<,0001*	Figure 7
Segment order	Abs Error / Distance	0,4615	<,0001*	Figure 9
Distance order	Error (mm)	0,4326	<,0001*	Figure 4
Distance order	Abs Error (mm)	0,4536	<,0001*	Figure 6
Distance order	Error / Distance	0,0544	0,4091	Figure 8
Distance order	Abs Error / Distance	-0,0520	0,4304	Figure 10

TABLE 3 Spearman’s rank-order correlation analysis.

18, 20, 23, 27, 32, 33) can impair the quality of the scan; performing a full-arch scan as a single operation can be more difficult than two separate halves, because, with the former strategy, the working field has to be kept dry and clean on both sides at the same time. If powder is needed, it can be even more challenging because saliva, tongue movements and cheeks can wash it out or make it “muddy”. For these reasons it is clinically easier to control one side of the arch at a time. We chose to set up an experiment similar to other ones (28, 30, 31) in order to collect new data comparable to

previous articles but, in addition, we measured distances between all the implants and not only between one and the other five. The rationale was to investigate if the loss of accuracy caused by error accumulation, documented along full-arches (28, 30, 31, 35), could affect measurements of similar lengths registered in different positions of the arch (e.g. 27-25, 13-15). As expected, linear error showed a tendency to increase with implant distance (Figure 4, 6) but, after dividing errors by their reference lengths and therefore obtaining standardised error ratios, we found that error ratio did not increase

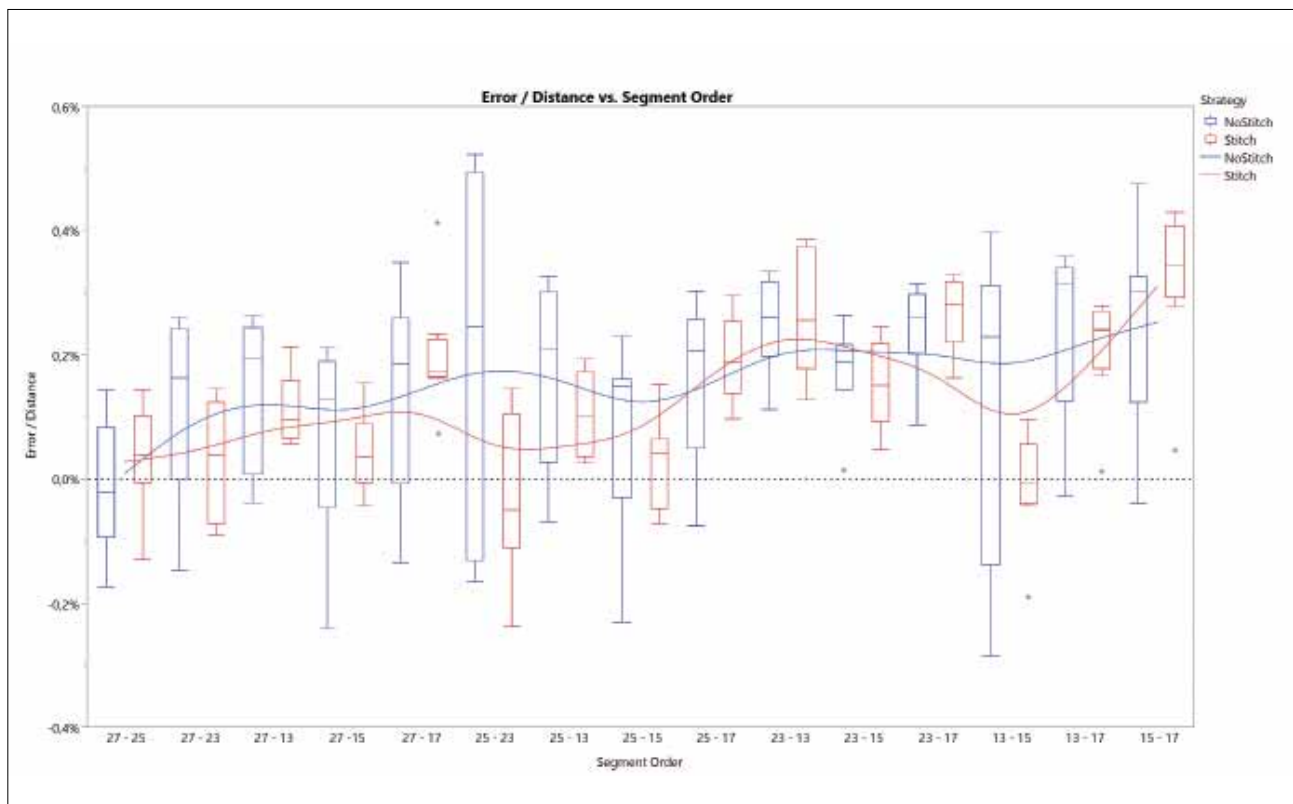


FIG. 7 Box plots and smoother lines (lambda = 0,05) illustrating errors as percentage of error / reference distance for each one of the fifteen segments measured. Segments are ordered from left quadrant to right quadrant. Interestingly, an increasing error percentage trend can be seen moving from left to right (from #27 to #17)

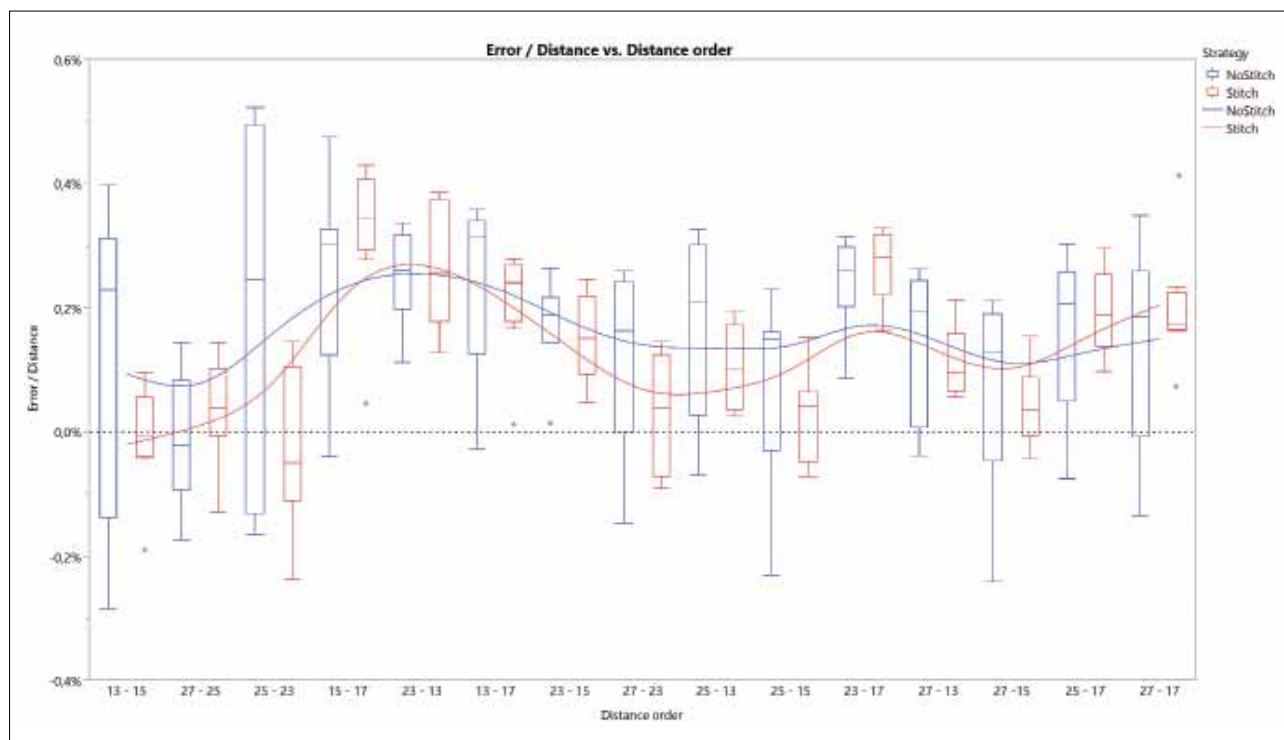


FIG. 8 Box plots and smoother lines ( $\lambda = 0,05$ ) illustrating errors as percentage of error/reference distance for each one of the fifteen segments measured. Segments are ordered from the shortest (13-15 = 11,577 mm) to the longest (27-17 = 46,599 mm). No trend can be seen between error percentage and segment length.

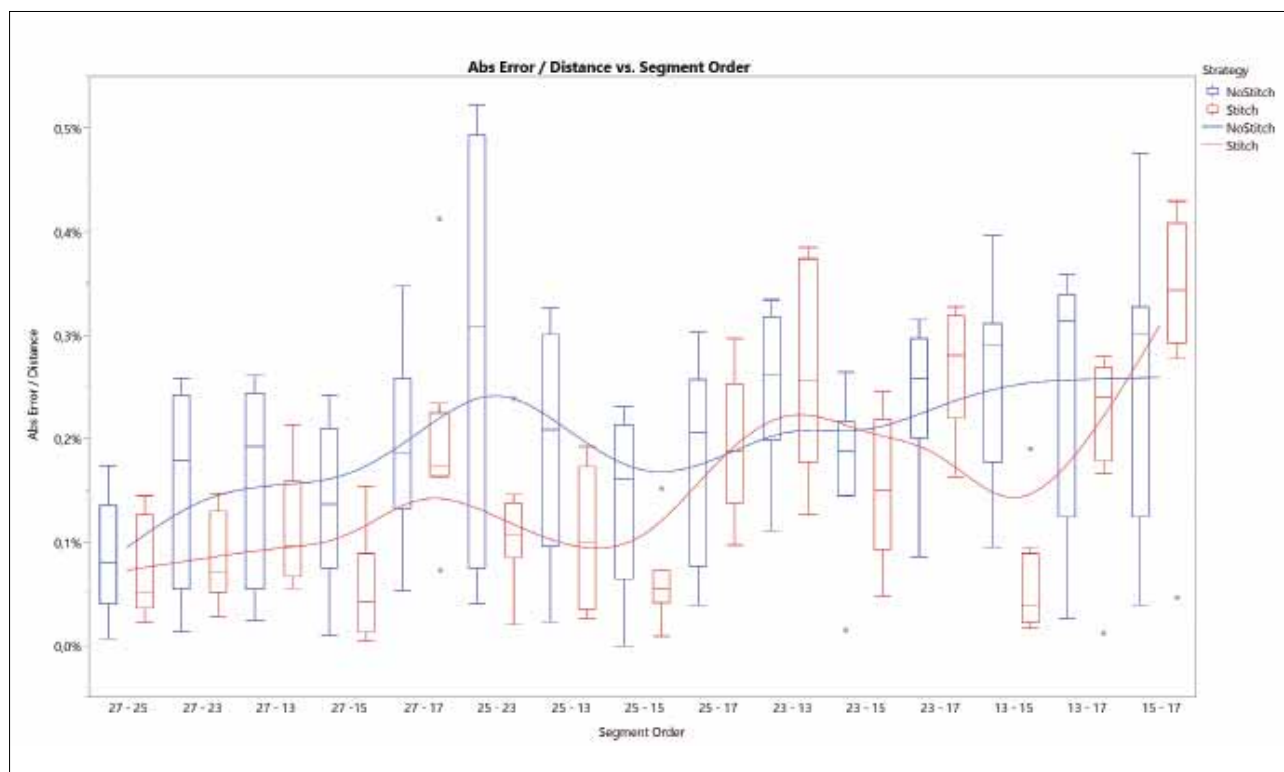
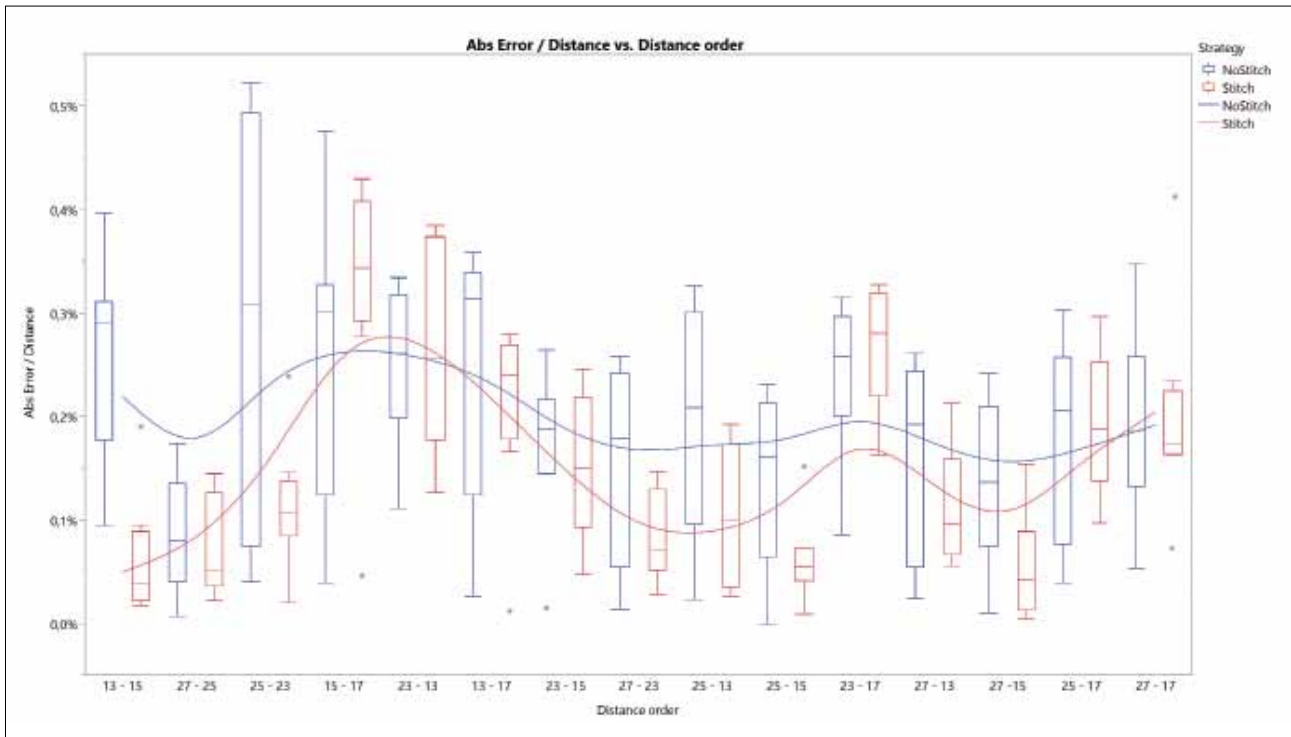


FIG. 9 Box plots and smoother lines ( $\lambda = 0,05$ ) illustrating absolute errors as percentage of absolute error/reference distance for each one of the fifteen segments measured. Segments are ordered from left quadrant to right quadrant. Like Figure 7, an increasing error percentage trend can be seen moving from left to right (from #27 to #17).



**FIG. 10** Box plots and smoother lines ( $\lambda = 0,05$ ) illustrating absolute errors as percentage of absolute error/reference distance for each one of the fifteen segments measured. Segments are ordered from left quadrant to right quadrant and from the shortest (13-15 = 11,577 mm) to the longest (27-17 = 46,599). No trend can be seen between error percentage and segment length.

with the distance between two implants (Figure 8, 10), but with implant position through the arch (Figure 7, 9). In fact, shifting toward the right side of the arch, errors increased and this correlation was statistically significant (Table 3). If only NS is considered, this behaviour could be explained with error propagation. Scanning always started from implant # 27 (left side of the arch) and moved toward # 17 (right side): if each error is added to a previous one, it is reasonable to expect an increase of the errors toward the end of the scan (right side of the mouth). However it is harder to fit this theory for the S strategy because one half-scan started from # 27 and the other one from # 17: we couldn't evaluate how the stitching algorithm works and it was not possible to evaluate if data processing could produce similar results to the NS strategy.

Another possible explanation, not investigated in the present study, could be related to the fact that implant angulations were different for each fixture and this affected the accuracy of the scan. In addition, it may not be possible to employ our method with all IOS systems. For example, CEREC (Dentsply-Sirona) allows the user to stop scanning, then continue, but requires the scan to be 'picked up' from a previously scanned anchor point. As such it would not be possible to commence each half-scan at the second molar region and meet in the contralateral canine region. Interestingly, a recent addition from this manufacturer is the 'Orthodontic 1.1' package,

which guides the user into performing sectional scans in a similar manner to the method described here. The manufacturers claim an enhanced accuracy for full arch scans and it would be interesting to explore this claim. One limitation of our study was that a post-hoc power analysis showed that it was underpowered to detect differences between the two strategies for each one of the segments: S and NS showed small differences, relatively high standard deviations and only segments 27-25, 13-15 reached a 0,8 power level.

## CONCLUSIONS

Stitch and No Stitch scanning protocols showed similar results in terms of linear scanning accuracy, and No Stitch showed a trend toward greater precision but the difference was not statistically significant. Our findings showed that a full-arch scan can be performed as separate pieces stitched together and clinicians may take advantage of this because saliva, tongue movements and tissues can be better controlled. Nevertheless, our findings have to be generalized with care and tested with other IOSs: we think they are closely related to the IOS used because different machines have different acquisition technologies, different algorithms to process raw data and different meshing procedures.

## Acknowledgements

We would like to thank Jockoo of Niang El Hadji Amadou and Eng. Davide Balduzzi for the precious technical support.

## REFERENCES

- Pjetursson BE, Thoma D, Jung R, Zwahlen M, Zembic A. A systematic review of the survival and complication rates of implant-supported fixed dental prostheses (FDPs) after a mean observation period of at least 5 years. *Clin Oral Implants Res* 2012;23 Suppl 6:22-38.
- Lee H, So JS, Hochstedler JL, Ercoli C. The accuracy of implant impressions: A systematic review. *J Prosthetic Dent* 2008;100:285-291.
- Stimmelmayer M, Beuer F, Edelhoff D, Güth J-F. Implant Impression Techniques for the Edentulous Jaw: A Summary of Three Studies. *J Prosthodont* 2015;25:146-150.
- Michaels GC, Carr AB, Larsen PE. Effect of prosthetic superstructure accuracy on the osteointegrated implant bone interface. *Oral Surg Oral Med Oral Pathol Oral Radiol Endod* 1997;83:198-205.
- Jemt T, Book K. Prosthesis misfit and marginal bone loss in edentulous implant patients. *Int J Oral Maxillofac Implants* 1996;11:620-625.
- Jemt T. Failures and complications in 391 consecutively inserted fixed prostheses supported by Branemark implants in edentulous jaws: a study of treatment from the time of prosthesis placement to the first annual checkup. *Int J Oral Maxillofac Implants* 1991;6:270-276.
- Buzayan MM, Yunus NB. Passive fit in screw retained multi-unit implant prosthesis understanding and achieving: a review of the literature. *J Indian Prosthodontic Society* 2013;14:16-23.
- Mormann WH. The evolution of the CEREC system. *J Am Dent Assoc* 2006;137 Suppl:75-135.
- Syrek A, Reich G, Ranftl D, Klein C, Cerny B, Brodesser J. Clinical evaluation of all-ceramic crowns fabricated from intraoral digital impressions based on the principle of active wavefront sampling. *J Dent* 2010;38:553-559.
- Seelbach P, Brueckel C, Wostmann B. Accuracy of digital and conventional impression techniques and workflow. *Clin Oral Investig* 2012.
- Brawek PK, Wolfart S, Endres L, Kirsten A, Reich S. The clinical accuracy of single crowns exclusively fabricated by digital workflow—the comparison of two systems. *Clin Oral Investig* 2013.
- Vennerstrom M, Fakhary M, Von Steyern PV. The fit of crowns produced using digital impression systems. *Swed Dent J* 2014;38:101-110.
- Nedelcu RG, Persson AS. Scanning accuracy and precision in 4 intraoral scanners: an in vitro comparison based on 3-dimensional analysis. *J Prosthet Dent* 2014;112:1461-1471.
- Pradies G, Zarauz C, Valverde A, Ferreira A, Martinez-Rus F. Clinical evaluation comparing the fit of all-ceramic crowns obtained from silicone and digital intraoral impressions based on wavefront sampling technology. *J Dent* 2015;43:201-208.
- Keul C, Stawarczyk B, Erdelt KJ, Beuer F, Edelhoff D, Guth JF. Fit of 4-unit FDPs made of zirconia and CoCr-alloy after chairside and labside digitalization—a laboratory study. *Dent Mater* 2014;30:400-407.
- Svanborg P, Skjerven H, Carlsson P, Eliasson A, Karlsson S, Ortorp A. Marginal and internal fit of cobalt-chromium fixed dental prostheses generated from digital and conventional impressions. *Int J Dentistry* 2014;2014:534382.
- Almeida e Silva JS, Erdelt K, Edelhoff D, Araujo E, Stimmelmayer M, Vieira LC, et al. Marginal and internal fit of four-unit zirconia fixed dental prostheses based on digital and conventional impression techniques. *Clin Oral Investig* 2014;18:515-523.
- Su TS, Sun J. Comparison of marginal and internal fit of 3-unit ceramic fixed dental prostheses made with either a conventional or digital impression. *J Prosthet Dent* 2016.
- Ueda K, Beuer F, Stimmelmayer M, Erdelt K, Keul C, Guth JF. Fit of 4-unit FDPs from CoCr and zirconia after conventional and digital impressions. *Clin Oral Investig* 2016;20:283-289.
- Flugge TV, Schlager S, Nelson K, Nahles S, Metzger MC. Precision of intraoral digital dental impressions with iTero and extraoral digitization with the iTero and a model scanner. *Am J Orthod Dentofacial Orthop* 2013;144:471-478.
- Naidu D, Freer TJ. Validity, reliability, and reproducibility of the iOC intraoral scanner: a comparison of tooth widths and Bolton ratios. *Am J Orthod Dentofacial Orthop* 2013;144:304-310.
- Ender A, Mehl A. Full arch scans: conventional versus digital impressions—an in-vitro study. *Int J Computerized Dentistry* 2011;14:11-21.
- Patzelt SB, Emmanouilidi A, Stampf S, Strub JR, Att W. Accuracy of full-arch scans using intraoral scanners. *Clin Oral Investig* 2014;18:1687-1694.
- Stimmelmayer M, Guth JF, Erdelt K, Edelhoff D, Beuer F. Digital evaluation of the reproducibility of implant scanbody fit—an in vitro study. *Clin Oral Investig* 2012;16:851-856.
- Lee SJ, Gallucci GO. Digital vs. conventional implant impressions: efficiency outcomes. *Clin Oral Implants Res* 2013;24:111-115.
- Joda T, Bragger U. Complete digital workflow for the production of implant-supported single-unit monolithic crowns. *Clin Oral Implants Res* 2014;25:1304-1306.
- Andriessen FS, Rijkens DR, van der Meer WJ, Wismeijer DW. Applicability and accuracy of an intraoral scanner for scanning multiple implants in edentulous mandibles: a pilot study. *J Prosthet Dent* 2014;111:186-194.
- Gimenez B, Ozcan M, Martinez-Rus F, Pradies G. Accuracy of a digital impression system based on parallel confocal laser technology for implants with consideration of operator experience and implant angulation and depth. *Int J Oral Maxillofac Implants* 2014;29:853-862.
- van der Meer WJ, Andriessen FS, Wismeijer D, Ren Y. Application of intraoral dental scanners in the digital workflow of implantology. *PLoS One* 2012;7:e43312.
- Gimenez B, Ozcan M, Martinez-Rus F, Pradies G. Accuracy of a digital impression system based on active wavefront sampling technology for implants considering operator experience, implant angulation, and depth. *Clin Implant Dent Relat Res* 2015;17 Suppl 1:e54-64.
- Gimenez B, Pradies G, Martinez-Rus F, Ozcan M. Accuracy of two digital implant impression systems based on confocal microscopy with variations in customized software and clinical parameters. *Int J Oral Maxillofac Implants* 2015;30:56-64.
- Boeddinghaus M, Breloer ES, Rehmann P, Wostmann B. Accuracy of single-tooth restorations based on intraoral digital and conventional impressions in patients. *Clin Oral Investig* 2015.
- Berredero S, Salido MP, Valverde A, Ferreira A, Pradies G. Influence of conventional and digital intraoral impressions on the fit of CAD/CAM-fabricated all-ceramic crowns. *Clin Oral Investig* 2016.
- Ender A, Mehl A. Influence of scanning strategies on the accuracy of digital intraoral scanning systems. *Int J Computerized Dentistry* 2013;16:11-21.
- Ender A, Attin T, Mehl A. In vivo precision of conventional and digital methods of obtaining complete-arch dental impressions. *J Prosthet Dent* 2016;115:313-320.